

MATHEMATICAL MODEL RESEARCH ON SUMMER COOLING CAPABILITY OF AN IMPROVED PASSIVE SOLAR HOUSE

Chuang Wang, Jinling Zhao, Bin Chen

School of Civil and Hydraulic Engineering, Dalian University of Technology, Dalian116024, China

ABSTRACT

For an improved passive solar house with built-in shutter and temperature control throttle joint measures, this paper used dynamic thermal network model and frequency domain regression analysis method, built the typical summer cooling overall coupling process of building dynamic thermal mathematical model.

KEYWORD: passive solar house, TCSW(thermal collector and storage wall), cooling, thermal property, thermal network model

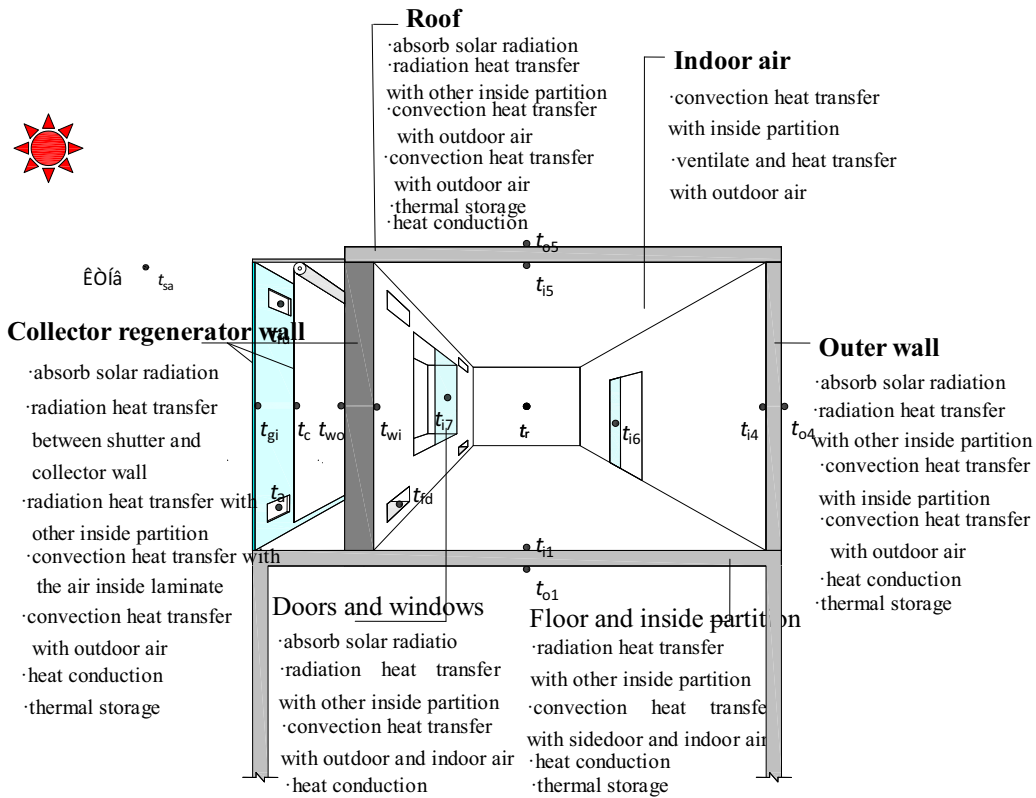
1. INTRODUCTION

Built-in shutter and temperature control throttle joint control is an effective measure to solve the traditional passive solar house in winter subcooling and summer overheat problems. It improves indoor thermal comfort of passive solar houses and promotes the positive significance of its application. For cooling condition in summer of an improved passive solar house with built-in shutter and temperature control measures, based on the previous thermal performance mathematical simulation of single collector and heat storage components, this paper used dynamic thermal network model and frequency domain regression analysis method, built and solved the overall coupling process of building dynamic thermal mathematical model, which was influenced by outdoor weather - air collector - storage enclosure / heat - indoor thermal environment. For further explore the optimization design of improved passive solar house and lay the foundation of operation control strategy, we would analyze the dynamic thermal performance of the improved passive solar houses.

2. THERMAL NETWORK MODEL

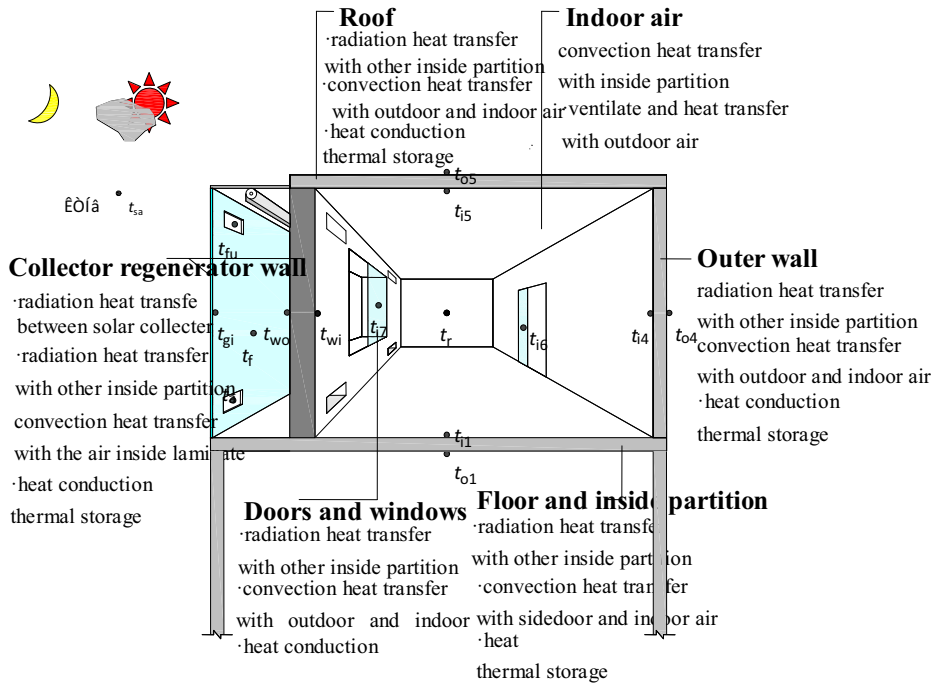
The cooling physical model of an improved passive solar house with built-in shutter and temperature control throttle joint measures is shown in Fig.1. Its typical cooling conditions are shutter shade during the clear day and ventilation during the night/ rainy day. The heat transfer process is a strong coupled mode among the non-state heat conduction, natural convection and surface radiation heat transfer; the regenerative effect of heavy envelope can't be ignored.

To Simplified analysis, we considered a range of assumptions in the calculation,for exemple: (1)uniform surface temperature of the envelope, indoor air temperature uniformity; (2)one-dimensional heat transfer process; (3)top and bottom of the air interlayer was insulate; (4)air temperature of the entrance to bottom of air interlayer was equal to the indoor air temperature; (5)air inside the interlayer was the one-dimensional flow along the vertical direction, ignored the pressure loss along the way; (6)ignored the latent heat of air, radiation absorption and heat penetration through the building envelope; (7)ignored internal disturbance;



a) Physical model of shutter shade during the clear day in summer

(control measures: put down shutter; open outer and internal below tuyere; close internal upper tuyere)



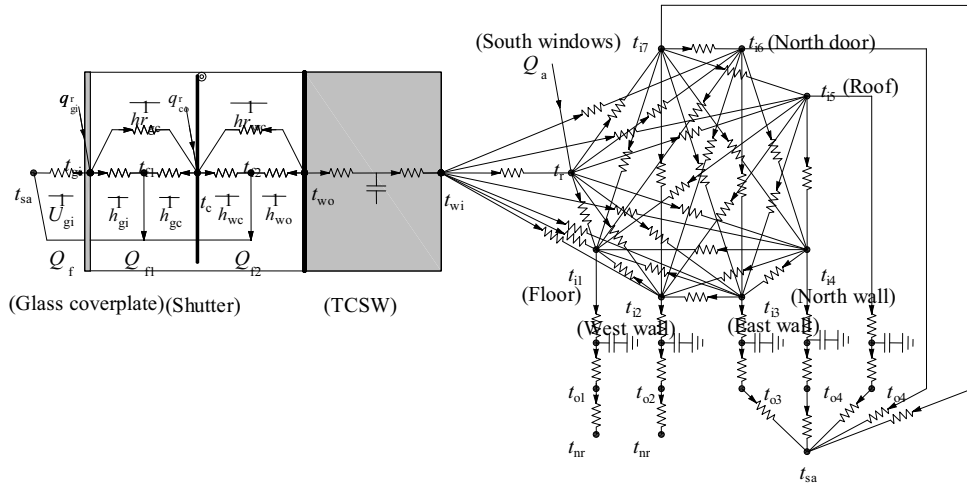
b) Physical model of ventilating during night or rainy day with low solar radiation

(control measures: roll up shutter; open outer and internal below tuyere; close internal upper tuyere)

Fig.1 Physical model of improved passive solar building

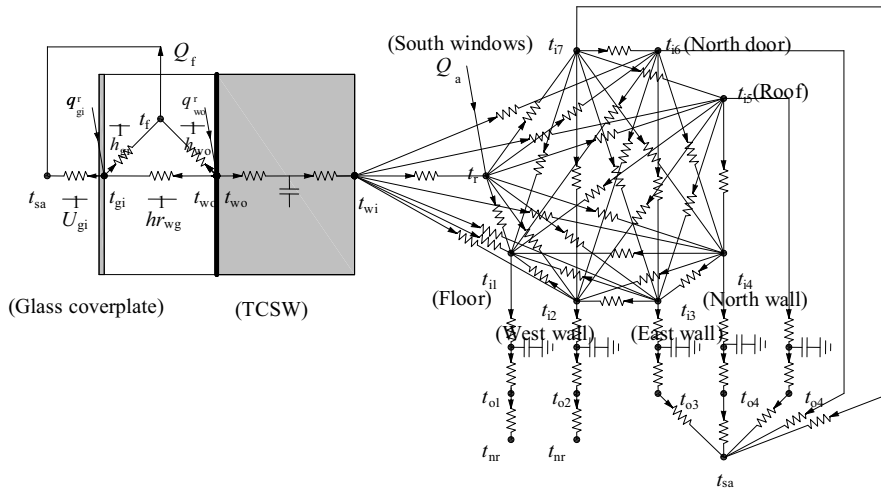
(8) solid material was homogeneous, and its physical parameters weren't changed with temperature;

Based on the above assumptions, the thermal resistance and heat capacity network model of typical cooling conditions for an improved passive solar house with built-in shutter and temperature control throttle joint measures was built, and it's shown in Fig.2.



a) network model of shutter shade during the clear day in summer

(control measures: put down shutter; open outer and internal below tuyere; close internal upper tuyere)



b) network model of ventilating during night or rainy day with low solar radiation

(control measures: roll up shutter; open outer and internal below tuyere; close internal upper tuyere)

Fig.2 network model of improved passive solar building

2. MATHEMATICAL MODEL

2.1 the corresponding heat balance equations of shutter shade condition

Took notice of the thermal resistance and heat capacity network model of shutter shade during the clear day in summer, air interlayer was divided into two vertical regions with opening side in this condition. The region between glass coverplate and shutter is interlayer I , and the region between TCSW and shutter is interlayer II . The heat balance equations per unit area of any nodes at τ moment are shown as followed:

For the internal surface of glass coverplate:

$$\alpha_i E(\tau) + hr_{g,c} [t_c(\tau) - t_{gi}(\tau)] = h_{gi} [t_{gi}(\tau) - t_{fi}(\tau)] + U_{gi} [t_{gi}(\tau) - t_{sa}(\tau)] \quad (1)$$

For the air in interlayer I :

$$h_{gi} A_{wo} [t_{gi}(\tau) - t_{fi}(\tau)] + h_{wo} A_c [t_c(\tau) - t_{fi}(\tau)] = Q_{fi}(\tau) \quad (2)$$

For thr shutter:

$$\tau_g \alpha_{co} E(\tau) + hr_{g,c} [t_{gi}(\tau) - t_c(\tau)] + hr_{w,c} [t_c(\tau) - t_{wo}(\tau)] = h_{co} [t_c(\tau) - t_{fi}(\tau)] + h_{ci} [t_c(\tau) - t_{f2}(\tau)] \quad (3)$$

For the air in interlayer II :

$$h_{wo} A_{wo} [t_{wo}(\tau) - t_{f2}(\tau)] + h_{ci} A_c [t_c(\tau) - t_{f2}(\tau)] = Q_{f2}(\tau) \quad (4)$$

In the equations, corner mark “n” is accordance with the envelope structure number appeared in fig.2(a), and it's same with the left text.

For the collector surface of TCSW:

$$hr_{w,c} [t_c(\tau) - t_{wo}(\tau)] = h_{wo} [t_{wo}(\tau) - t_{f2}(\tau)] + \sum_{j=0}^N X(j) t_{wo}(\tau - j) - \sum_{j=0}^N Y(j) t_{wi}(\tau - j) \quad (5)$$

For the indoor air:

$$h_{wi} A_{wi} [t_{wi}(\tau) - t_r(\tau)] + \Phi_a(\tau) = \sum_{n=1}^7 h_{wn} A_n [t_{in}(\tau) - t_r(\tau)] \quad (6)$$

For the internal surface of TCSW:

$$\sum_{j=0}^N Y(j) t_{wo}(\tau - j) - \sum_{j=0}^N Z(j) t_{wi}(\tau - j) = h_{wi} [t_{wi}(\tau) - t_r(\tau)] + \sum_{n=1}^6 hr_{w,n} [t_{wi}(\tau) - t_{in}(\tau)] \quad (7)$$

For the internal surface of heavy envelope except TCSW:

$$q_{in}^i(\tau) + hr_{w,n} [t_{wi}(\tau) - t_{in}(\tau)] + \sum_{k=1}^7 hr_{n,k} [t_{ik}(\tau) - t_{in}(\tau)] + h_{wn} \left[t_r(\tau) - t_{in}(\tau) = \sum_{j=0}^N Z_n(j) t_{in}(\tau - j) - \sum_{j=0}^N Y_n(j) t_{on}(\tau - j) \right] \quad (8)$$

In the equations, the internal surface corner mark n=1,2,3,4,5.

For the internal surface of Lightweight envelope:

$$q_{in}^r(\tau) + hr_{w,n}[t_{wi}(\tau) - t_{in}(\tau)] + \sum_{k=1}^7 hr_{n,k}[t_{ik}(\tau) - t_{in}(\tau)] + h_{wn}[t_r(\tau) - t_{in}(\tau)] = U_{in}[t_{in}(\tau) - t_{sa}(\tau)] \quad (9)$$

In the equations, the internal surface corner mark n=6,7,8.

For the external surface of heavy envelope except TCSW:

$$q_{on}^r(\tau) = h_{wind}[t_{on}(\tau) - t_{sa}(\tau)] + \sum_{j=0}^N X_n(j)t_{on}(\tau - j) - \sum_{j=0}^N Y_n(j)t_{in}(\tau - j) \quad (10)$$

The improved composition of passive solar house in winter sunny day air thermal cycling conditions of the heat balance equations for improved passive solar house thermal cycling in winter clear day are made up by equation1~10.

For the air mass flow rate in the interlayer:

$$m = \rho_f C_d \left(A_{fu} A_{fd} / \sqrt{A_{fu} + A_{fd}} \right) \sqrt{2g L_w (t_{fu} - t_r) / (t_r + 273)} \quad (11)$$

To determined the air temperature at the top outlet of interlayer, we would built the heat balance equations for air unit in the interlayer:

$$m C_p dt_f / dy \delta y = [h_{gi}(t_{gi} - t_f) + h_{wo}(t_{wo} - t_f)] W \delta y \quad (12)$$

Integrated the equation (12), and we would obtain the air temperature at the top outlet of interlayer:

$$t_{fu} = t_r e^{-\beta L_w} + (1 - e^{-\beta L_w}) \gamma / \beta = t_r e^{-\beta L_w} + (h_{wo} t_{wo} + h_{gi} t_{gi} / h_{wo} + h_{gi})(1 - e^{-\beta L_w}) \quad (13)$$

In the equation, $\beta = (h_{gi} + h_{wo})W / m C_p$, $\gamma = (h_{gi} t_{gi} + h_{wo} t_{wo})W / m C_p$.

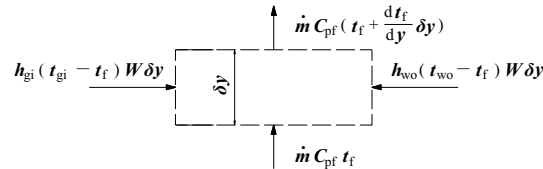


Fig.3 heat balance for unit in the air flow direction of interlayer

2.2 the corresponding heat balance equations of non-shutter shade condition

According to the thermal network model shown in the figure.2.b, we built the heat balance equation for each node of the improved passive solar house during summer night or rainy day at low solar radiation.

For the internal surface of glass coverplate:

$$\alpha_i E(\tau) + hr_{w,g}[t_{wo}(\tau) - t_{gi}(\tau)] = h_{gi}[t_{gi}(\tau) - t_f(\tau)] \quad (14)$$

For the air in interlayer:

$$h_{gi}[t_{gi}(\tau) - t_f(\tau)] + h_{wo}[t_{wo}(\tau) - t_f(\tau)] = Q_f(\tau) / A_{wo} \quad (15)$$

For the collector surface of TCSW:

$$\tau_g \alpha_w E(\tau) = hr_{w,g} [t_{wo}(\tau) - t_{gi}(\tau)] + h_{wo} \left[t_{wo}(\tau) - t_r(\tau) + \sum_{j=0}^N X(j) t_{wo}(\tau - j) - \sum_{j=0}^N Y(j) t_{wi}(\tau - j) \right] \quad (16)$$

For the indoor air:

$$h_{wi} A_{wi} [t_{wi}(\tau) - t_r(\tau)] + Q_a(\tau) = \sum_{n=1}^7 h_{wn} A_n [t_{in}(\tau) - t_r(\tau)] \quad (17)$$

For the internal surface of TCSW:

The heat balance equation is similar with formula 4.23, which for air thermal cycling conditions during the winter,

$$\sum_{j=0}^N Y(j) t_{wo}(\tau - j) - \sum_{j=0}^N Z(j) t_{wi}(\tau - j) = h_{wi} [t_{wi}(\tau) - t_r(\tau)] + \sum_{n=1}^6 hr_{w,n} [t_{wi}(\tau) - t_{in}(\tau)] \quad (18)$$

For the internal surface of heavy envelope except TCSW:

$$\begin{aligned} q_{in}^r(\tau) + hr_{w,n} [t_{wi}(\tau) - t_{in}(\tau)] + \sum_{k=1}^7 hr_{n,k} [t_{ik}(\tau) - t_{in}(\tau)] + h_{wn} [t_r(\tau) - t_{in}(\tau)] \\ = \sum_{j=0}^N Z_n(j) t_{in}(\tau - j) - \sum_{j=0}^N Y_n(j) t_{on}(\tau - j) \end{aligned} \quad (19)$$

In the equations, the internal surface corner mark n=1,2,3,4,5.

For the internal surface of Lightweight envelope:

$$\begin{aligned} q_{in}^r(\tau) + hr_{w,n} [t_{wi}(\tau) - t_{in}(\tau)] + \sum_{k=1}^7 hr_{n,k} [t_{ik}(\tau) - t_{in}(\tau)] + h_{wn} [t_r(\tau) - t_{in}(\tau)] \\ = U_{in} [t_{in}(\tau) - t_{sa}(\tau)] \end{aligned} \quad (20)$$

In the equations, the internal surface corner mark n=6,7,8.

For the external surface of heavy envelope except TCSW:

We would build heat balance equations for the external surface of wall, including east wall, west wall, north wall, floor and roof, the heat balance equation is similar with formula 4.34,

$$q_{on}^r(\tau) = h_{wind} [t_{on}(\tau) - t_{sa}(\tau)] + \sum_{j=0}^N X_n(j) t_{on}(\tau - j) - \sum_{j=0}^N Y_n(j) t_{in}(\tau - j) \quad (21)$$

In the equations, the internal surface corner mark n=1,2,3,4,5.

According to the formula 14~21, we would obtain the heat balance equation for thermal insulation shutter of the improved passive solar house during night/rainy day in the winter.

2.2 determine the coefficient of heat balance equation

In the above equations, frequency domain regression analysis method(FDR), which is based on system identification theory, was used to calculate the reaction coefficient $X(j)$, $Y(j)$, $Z(j)$ of unsteady state heat conduction; the coverplate was hollow double-glazed glass in the radiation term, and absorb rate of the intimal glass was calculated by ray tracing method; the solar radiation heat flux q_{in} , which is absorbed by the internal surface of level i envelope, was calculated by the definite sunshine movement simulate process.

For the convective heat transfer coefficient of internal surface of the glass coverplate:

$$h_{gi} = Nu_g \lambda_{fg} / L_g \quad (22)$$

In the equations, L_g is the height of the glass cover, m; Nu_g is the nusselt number of glass cover side in the air interlayer and λ_{fg} is the heat conduction coefficient, $W/(m^2 \cdot ^\circ C)$.

For the convective heat transfer coefficient of external surface of the shutter:

$$h_{co} = Nu_g \lambda_{fg} / L_c \quad (23)$$

In the equations, L_g is the height of the shutter, m; Nu_g is the nusselt number of glass cover side in the air interlayer and λ_{fg} is the heat conduction coefficient, $W/(m^2 \cdot ^\circ C)$.

For the convective heat transfer coefficient of internal surface of the shutter:

$$h_{ci} = Nu_w \lambda_{fw} / L_c \quad (24)$$

In the equations, L_g is the height of the shutter, m; Nu_g is the nusselt number of collector wall side in the air interlayer and λ_{fg} is the heat conduction coefficient, $W/(m^2 \cdot ^\circ C)$.

For the convective heat transfer coefficient of collector wall side of TCSW:

$$h_{wo} = Nu_w \lambda_{fw} / L_w \quad (25)$$

In the equations, L_g is the height of TCSW, m; Nu_g is the nusselt number of collector wall side in the air interlayer and λ_{fg} is the heat conduction coefficient, $W/(m^2 \cdot ^\circ C)$.

In the above equations, the nusselt number Nu_g (for the glass cover side in the close interlayer) and Nu_w (for the collector wall side in the close interlayer) was counted by following case.

When $Gr_g \& Gr_w \leq 2860$, $Nu_g \& Nu_w = 1$, and the heat transfer process in the interlayer is pure heat conduction process;

When $8.6 \times 10^3 < Gr_g \& Gr_w < 2.9 \times 10^5$, $Nu_g \& Nu_w = 0.197(Gr_w Pr_w)^{1/4} (L_m/d_w)^{-1/9}$;

When $2.9 \times 10^5 < Gr_g \& Gr_w < 1.6 \times 10^7$, $Nu_g \& Nu_w = 0.073(Gr_w Pr_w)^{1/3} (L_m/d_w)^{-1/9}$,

And the mean temperature $t_{wm} = (t_c + t_{gi})/2$, $t_{wm} = (t_c + t_{wo})/2$; the mean length is the gap d_g between shutter and glass cover, and the gap d_w between shutter and collector wall side.

According to the document[11], we would obtain the solar radiation heat flux q_{in} , which is absorbed by the external surface of the heavy envelope, and the convective heat transfer coefficient, the radiant heat transfer coefficient, the physics parameter and the rule number appeared in the above equations.

3. PROVE OF MATHEMATICAL MODEL

Draw up computer program, which was built by Gauss iteration, was used to solve the above heat balance equations. It is shown in Figure 4.

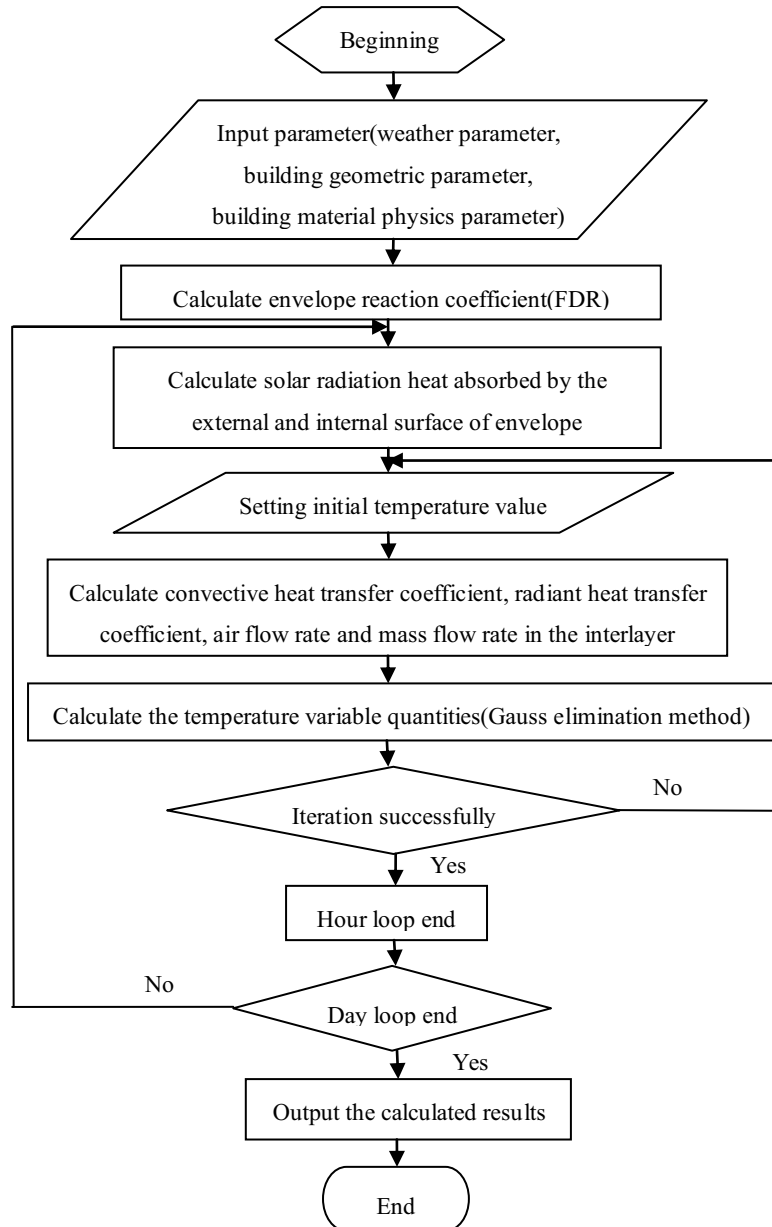


Fig.4 Flow chart of calculation

The mathematical model results were compared with test results, which was proceeded in the entity large passive solar laboratorial house with built-in shutter and temperature control throttle joint measures. The passive solar experimental house is located in DLUT. The geometry size is $3.9 \times 3.9 \times 2.8 \text{m}^3$. The coverplate is hollow double-glazed glass, southing heavy envelope is 300mm thick concrete wall, the net wide is 900mm and the collector surface is spreaded on dark green thermal absorb paintcoat. The other orientations walls is 300mm thick hollow concrete cinder block added 100mm benzol insulating layer, and the roof is 80mm

thick concrete block added 100mm benzol insulating layer. The outlet size of interlayer is 150×170mm and it has adiabatic shutter inside the interlayer. The test time is July. During the experiment, open the temperature control damper and roll down the shutter to get the shade effects in the daytime; closed the temperature control damper and roll down the shutter to get the insulation effects in the night. In the experiment, we used couple devices to record the data, such as computer circuit detection system, SERIES EE66 wind speed meter, PC-2 solar radiation recorder, mini outdoor weather station and so on. The 28 indoor air temperature measuring points was layout according to the grid, and the average temperature of any dot was taken as indoor air temperature t_r . The measuring points' position on the TCSW is shown in Figure 5.

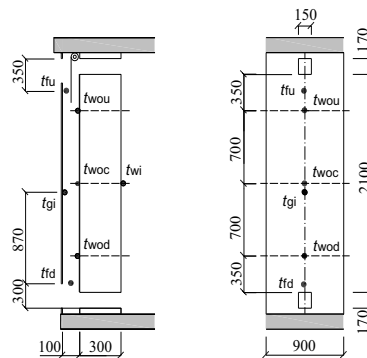
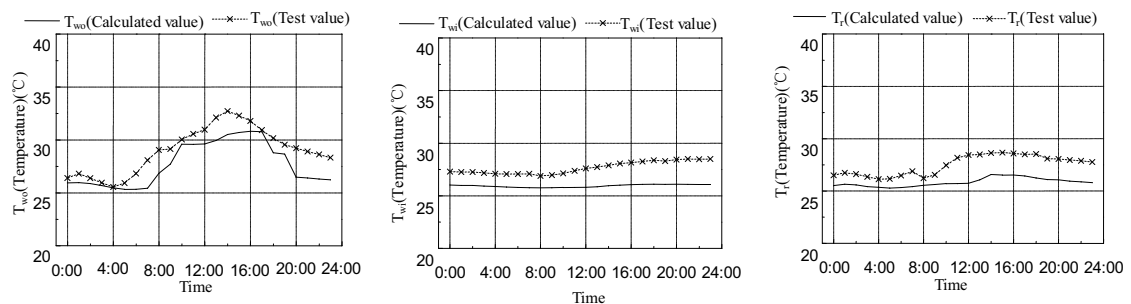


Fig.5 Location of temperature probes in Trombe wall

By this arrangement, we could gain the internal surface temperature of the coverplate t_{gi} , internal surface temperature t_{wi} of the wall t_{wi} , the upper and lower outlet air temperature of the interlayer t_{fu} and t_{fd} , the upper, middle and lower surface temperature of the collector wall t_{wou} , t_{woc} and t_{wod} . The average temperature of the three measuring points on collector surface was the collector surface temperature t_{wo} .



a) comparison of collector surface temperature t_{wo} b) comparison of internal surface temperature t_{wi} c) comparison of indoor air temperature t_r

Fig.6 Comparison of tested data and calculated data under passive ventilation in summer

Put construction geometry size of the experimental house, physical parameters of the materials and outdoor meteorological parameters during the experiment as input values into the computer program to solve the equations. For the heating conditions in winter, the compare curve between calculated and experimental values of each node temperature of the improved passive solar house is shown in Figure 6.

Deviation analysis for the calculated and experimental values, average absolute difference

$\sigma_{abs} = (1/n) \sum_1^n |t_{ca} - t_{ob}|$ and average relative error $\sigma_{avg} = (1/n) \sum_1^n (t_{ca}/t_{ob} - 1)$ is used for the deviation

indicator, in the equation, t_{ca} is the calculated value and t_{ob} is the experimental value. According to the analysis, average absolute difference of t_r was 2.17°C, average relative error was -7.82%; average absolute difference of t_{wo} was 2.98°C, average relative error was -9.84%; average absolute difference of t_{wi} was 2.24°C, average relative error was -8.05%. Due to the weather conditions and laboratory personnel varied, the implementary time of control measures was changed during the experiment, and the deviation was happened. Nevertheless, the implementary time of control measures was constant for the mathematical model. Under the assume of mathematical model, we ignored the air infiltration losses of doors and windows, heat transfer between the outdoor environment and top and bottom layer of the interlayer was ignored. The deviations between each calculated and experimental temperature values were below 10%, which was shown that the simulation results and experimental values could be matched well. Then, we could say the mathematical model established in this text was feasible.

4. Conclusion

In this paper, used dynamic thermal network model and frequency domain regression analysis method, we built a dynamic thermal process model of the typical heating conditions to whole building for an improved passive solar house with built-in shutter and temperature control measures. Every factor was considered for the model, such as, outdoor meteorological factors, non-state heat conduction of compound wall, natural convection heat transfer inside the open flank interlayer and closed interlayer, the solar radiation onto the surface of envelope. The Simulation results and test results of physical experimental house could be fit well, which was Verified the accuracy of the mathematical model.

Symbol table

A_{fd} — bottom outlet area of interlayer, m^2
 A_{fu} — top outlet area of interlayer, m^2
 A_{wo} — collector surface area of TCSW, m^2
 A_{wi} — collector surface area and internal surface of TCSW, m^2
 A_n — internal surface area of envelop besides TCSW, m^2
 A_i — temperature wave amplitude of internal surface of wall, °C
 A_o — temperature wave amplitude of wall surface, °C
 C_d — air effluent coefficient in the interlayer
 C_p — air specific heat capacity in the interlayer, $kJ/(kg \cdot ^\circ C)$
 d — thickness of the air interlayer, m
 d_g — gap between coverplate and shutter, m
 d_w — gap between TCSW and shutter, m
 F — solar irradiance, W/m^2

g — air gravity, m/s^2
 h_{gi} — convection heat transfer coefficient of inner surface of glass coverplate, $W/(m^2 \cdot ^\circ C)$
 h_{gc} — equivalent heat transfer coefficient between glass coverplate and shutter, $W/(m^2 \cdot ^\circ C)$
 h_{wc} — equivalent heat transfer coefficient between TCSW and shutter, $W/(m^2 \cdot ^\circ C)$
 h_{wo} — convection heat transfer coefficient of collector surface of TCSW, $W/(m^2 \cdot ^\circ C)$
 h_{wi} — convection heat transfer coefficient of inner surface of TCSW, $W/(m^2 \cdot ^\circ C)$
 h_{wind} — convection heat transfer coefficient of exterior surface of envelop caused by wind, $W/(m^2 \cdot ^\circ C)$
 h_{wn} — convection heat transfer coefficient of inner surface of envelop besides TCSW, $W/(m^2 \cdot ^\circ C)$
 $h_{r_{g,c}}$ — radiation heat transfer coefficient between glass coverplate and shutter, $W/(m^2 \cdot ^\circ C)$
 $h_{r_{w,c}}$ — radiation heat transfer coefficient between TCSW and shutter, $W/(m^2 \cdot ^\circ C)$
 $h_{r_{n,k}}$ — radiation heat transfer coefficient between inner surface of envelop besides TCSW, $W/(m^2 \cdot ^\circ C)$
 $h_{r_{v,g}}$ — radiation heat transfer coefficient between glass coverplate and TCSW, $W/(m^2 \cdot ^\circ C)$
 $h_{r_{v,n}}$ — radiation heat transfer coefficient between inner surface of other envelop and inner surface of TCSW, $W/(m^2 \cdot ^\circ C)$
 L_w — height of TCSW, m
 m — air mass flow rate in the interlayer, kg/s
 q_{in}^r — solar radiation heat flux absorbed by inner surface of envelope besides TCSW, W/m^2
 q_{on}^r — solar radiation heat flux absorbed by exterior surface of heavy envelope besides TCSW, W/m^2
 Q_f — air heat flow rate in the interlayer, W
 t_c — shutter temperature, $^\circ C$
 t_f — air temperature in the interlayer, $^\circ C$
 t_{fu} — outlet air temperature in the top of interlayer, $^\circ C$
 t_{gi} — inner surface temperature of glass coverplate, $^\circ C$
 t_{in} — inner surface temperature of other envelop besides TCSW, $^\circ C$
 t_{on} — exterior surface temperature of other envelop besides TCSW, $^\circ C$
 t_r — indoor air temperature, $^\circ C$
 t_{sa} — multiple environment temperature, $^\circ C$
 t_{wo} — collector surface temperature of TCSW, $^\circ C$
 t_{wi} — collector and inner surface temperature of TCSW, $^\circ C$
 U_{gi} — multiple heat transfer coefficient between glass coverplate and environment, $W/(m^2 \cdot ^\circ C)$
 U_{in} — multiple heat transfer coefficient between environment and door(window), $W/(m^2 \cdot ^\circ C)$
 W — width of TCSW, m
 α_i — absorb rate of inner surface of glass coverplate, %
 α_w — absorb rate of collector surface of TCSW, %
 α_{co} — absorb rate of exterior surface of shutter, %
 λ_{fg} — air thermal conductivity of glass coverplate side in the interlayer, $W/(m^2 \cdot ^\circ C)$
 λ_{fw} — air thermal conductivity of TCSW side in the interlayer, $W/(m^2 \cdot ^\circ C)$
 ρ_f — air density in the interlayer, kg/m^3

$X(j)$, $X_n(j)$ —endothermic reaction coefficient of collector surface of TCSW and exterior surface of level n heavy envelope, $W/(m^2 \cdot ^\circ C)$

$Y(j)$, $Y_n(j)$ —heat transfer reaction coefficient of TCSW and level n heavy envelope, $W/(m^2 \cdot ^\circ C)$

$Z(j)$, $Z_n(j)$ —endothermic reaction coefficient of inner surface of TCSW and inner surface of level n heavy envelope, $W/(m^2 \cdot ^\circ C)$

Gr_g , Gr_w —Grashof Number of glass coverplate side and TCSW side in the interlayer

Nu_g , Nu_w —Nusselt Number of glass coverplate side and TCSW side in the interlayer

Pr_g , Pr_w —Prandtl Number of glass coverplate side and TCSW side in the interlayer

References

- [1] Jinling Zhao, Bin Chen, Yinghui Ding et al, 2005. Ventilation mode study of new Trombay wall passive cooling at maritime climate conditions[J]. Heating, Ventilating and Air Conditioning, 35(8): 10–15.
 - [2] Bin Chen, Xing Chen, Yinghui Ding, Huijuan chen et al, 2006. Influence to thermal performance of Trombay wall built-in shutter at winter[J]. Acta Energiæ Solaris Sinica, 27(16): 564–570.
 - [3] Hong Ye, Xingshi Ge, 2000. Dynamic simulation and thermal performance comparison of several collectors - thermal storage wall solar house[J]. Acta Energiæ Solaris Sinica, 21(4): 349–357.
 - [4] Ren M J, Wright J A, 1998. A ventilated slab thermal storage system model[J]. Building and Environment, 33(1): 43–52.
 - [5] Li Yuguo. Analysis of natural ventilation—A summary of existing analytical solutions[R]. International energy, Energy conservation in buildings and community systems, Technical TR12
 - [6] Youming Chen, 2004. New non-steady heat transfer analysis method of building envelope[M], Science Press, Beijing
 - [7] Ximin Zhang, Zepei Ren, Feiming Mei, 1993. Heat Transfer[M], China Building Project Press, Beijing
 - [8] Qinsen Yan, Qingzhu Zhao, 1986. Building thermal process[M], China Building Project Press, Beijing
 - [9] Buxuan Wang, 2002. Engineering heat and mass transfer[M], Science Press, Beijing
 - [10] Shiming Yang, Wenquan Tao, 1998. Heat Transfer(Third Edition)[M], Higher Education Press, Beijing
 - [11] Bansal N K, Mathur Jyotirmay, Mathur Saniay et al, 2005. Modeling of window-sized solar chimneys for ventilation[J]. Building and Environment, 40(10): 1302–1308.
 - [12] Meteorological Library of Meteorological Information Center in China Meteorological Administration, Building Technology Science Department of Tsinghua University, 2006. Specific meteorological data sets for China building thermal environment analysis[M], China Building Industry Press, Beijing
 - [13] Jinling Zhao, Bin Chen, Yongxue Wang et al, 2008. Dynamic thermal performance study of passive solar heating system [J]. Academic journal of DLUT, 48(4): 580–586.
 - [14] Bouchair A, 1988. Moving air using stored solar energy[C]. Proceedings of 13th National Passive Solar Conference, Massachusetts: Cam-bridge, 33–38.
 - [15] Chen Z D, P Bandopadhyay, J Halldorsson et al, 2003. An experimental investigation of a solar chimney with uniform heat flux[J]. Building and Environment, 38(7): 893–906.
-